Unexpected Acceleration of Type 1 Diabetes by Transgenic Expression of B7-H1 in NOD Mouse Peri-Islet Glia

Jason Yantha,[1,2] Hubert Tsui,[1,2] Shawn Winer,[1,2] Aihua Song,[1,2] Ping Wu,[1,2] Geoff Paltser,[1,2] James Ellis,[3] and H.-Michael Dosch[1,2]

OBJECTIVE—Autoimmune target tissues in type 1 diabetes include pancreatic β-cells and peri-islet Schwann cells (pSC)—the latter active participants or passive bystanders in pre-diabetic autoimmune progression. To distinguish between these alternatives, we sought to suppress pSC autoimmunity by transgenic expression of the negative costimulatory molecule B7-H1 in NOD pSC.

RESEARCH DESIGN AND METHODS—A B7-H1 transgene was placed under control of the glial fibrillary acidic protein (GFAP) promoter. Transgenic and wild-type NOD mice were compared for transgene PD-1 affinities, diabetes development, insulitis, and pSC survival. Mechanistic studies included adoptive type 1 diabetes transfer, B7-H1 blockade, and T-cell autoreactivity and sublineage distribution.

RESULTS—Transgenic and endogenous B7-H1 bound PD-1 with equal affinities. Unexpectedly, the transgene generated islet-selective CD8^{+} bias with accelerated rather than suppressed diabetes progression. T-cells of diabetic transgenics transferred type 1 diabetes faster. There were no earlier pSC losses due to conceivable transgene toxicity, but transgenic pSC loss was enhanced by 8 weeks, preceded by elevated GFAP autoreactivity, with high-affinity T-cells targeting the major NOD K[d]-GFAP epitope, p253–261. FoxP3^{+} regulatory T- and CD11c^{+} dendritic cell pools were unaffected.

CONCLUSIONS—In contrast with transgenic B7-H1 in NOD mouse β-cells, transgenic B7-H1 in pSC promotes rather than protects from type 1 diabetes. Here, ectopic B7-H1 enhanced the pathogenicity of effector T-cells, demonstrating that pSC can actively impact diabetes progression—likely through modification of intraislet T-cell selection. Although pSC cells emerge as a new candidate for therapeutic targets, caution is warranted with regard to the B7-H1–PD1 axis, where B7-H1 overexpression can lead to accelerated autoimmune disease. *Diabetes* **59:2588–2596, 2010**

The NOD mouse is a spontaneous model of type 1 diabetes, with genetic and pathophysiological roots comparable with the human disease (1). Pancreatic islets of Langerhans are tightly enveloped by peri-islet Schwann cells (pSC) that express glial fibrillary acidic protein (GFAP), a marker of Schwann cells and astrocytes (2). During pre-diabetes progression, T-cell infiltrates accumulate at the endo-crine/exocrine border, constituted by the pSC mantle, where lengthy "peri"-insulitis lasts for weeks to months in NOD mice and likely for years in humans with islet autoimmunity. Eventual breakdown of the pSC mantle initiates pathogenic islet invasion, progressive β-cell loss, insulin deficiency, and overt diabetes development. In NOD mice, CD8^{+} T-cells predominate islet attack until late in this process (3).

Islet T-cell infiltrations are heterogeneous in their target autoantigen specificities for not only β-cell–selective autoantigens (e.g., insulin) but also autoantigens shared by β-cells and nervous system tissue, islet-associated autoantigens shared by pSC and β-cells (e.g., S100β) or those that are pSC specific (e.g., GFAP) (4). pSC functions and their importance in type 1 diabetes development have yet to be fully characterized. In NOD mice, pSC-specific T-cell autoreactivities are present by 5 weeks of age. GFAP target epitopes were recently mapped to residues 79–87 and 253–261 for K[d] and 96–110, 116–130, and 216–230 for NOD-IA[g7], and fresh ex vivo CD8^{+} cells mediate direct lysis of primary pSC cultures from diabetic NOD mice (5).

pSC cells likely have physiological functions similar to conventional Schwann cells of the peripheral nervous system, providing neurotrophic support for islet-innervating neurons as well as the neural crest-derived β-cell (2). For example, nerve growth factor, glial cell—derived neurotrophic factor, and insulin-like growth factor-1 promote β-cell survival and probably regeneration (6–8). Loss of these factors with pSC destruction may amplify β-cell stress, enhancing β-cell susceptibility to inflammatory insults (7). Anatomically, pSC provide a physical barrier to infiltrating T-cells, accumulating at the endo-exocrine islet border and impeding direct β- and T-cell contact.

B7-H1, a ligand for programmed death (PD)-1, is expressed by CD4^{+} and CD8^{+} T-cells, B-cells, dendritic cells (DCs), macrophages, mast cells, and nonhemopoietic tissues (9). In nonlymphoid tissue, DC-B7-H1 supports peripheral tolerance, limiting randomly arising autoaggressive lymphocytes and their inflammatory tissue damage (10,11). In tumors, expression of B7-H1 contributes to
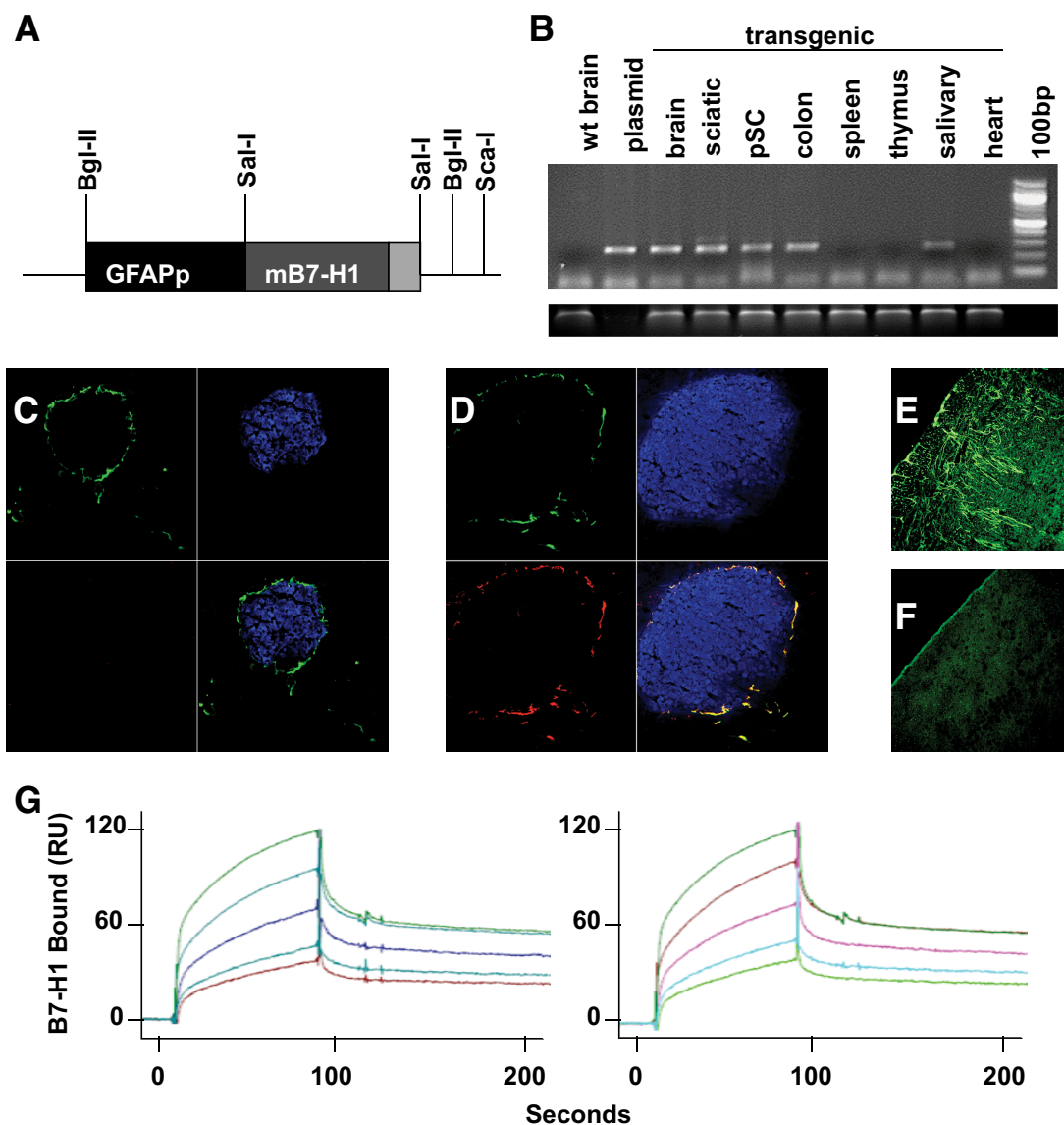
FIG. 1. B7–H1 transgene construct and expression. *A*: Construct map with GFAP promoter (GFAPp), restriction sites, and poly-A region (gray). *B*: Transgene-specific RT-PCR (see RESEARCH DESIGN AND METHODS) in various tissues. *Lower lane*: cDNA calibration controls (glucuronidase). B7–H1 transcripts were detectable in brain, sciatic nerve, purified and cultured pSC, colon, and salivary gland. *C* and *D*: Confocal fluorescent microscopy of wild-type NOD (*C*) and GFAP-tg (*D*) pancreas sections stained for insulin (blue), GFAP (green), and B7–H1 (red). pSC expression of B7–H1 was only detected in transgenics, coexpressed with GFAP (yellow). *E* and *F*: B7–H1 protein expression (green) was abundant in transgenic brain tissue (*E*), with only weak autofluorescence in brain tissue edges of wild-type (wt) controls (*F*). *G*: Biacore analysis of transgenic (*left panel*) vs. endogenous B7–H1 wild type (*right panel*) revealed near-identical affinities with the PD-1 receptor (*G*) (Table 1). (A high-quality digital representation of this figure is available in the online issue.)

immune evasion, inducing anergy or apoptosis of tumor-specific T-cells (12–14). Consistently with an inhibitory role, treatment of NOD mice with blocking antibodies to either PD-1 or B7-H1 accelerates diabetes (15), with analogous scenarios in autoimmune (16) and other (12,17,18) models. These systemic manipulations of the PD-1/B7-H1 axis generated the consensus view that B7-H1 ligation keeps potentially damaging autoimmune T-cells in check and serves to downregulate lymphoid effector functions (19).

However, conflicting data exist. The B7-H1 pathway can promote T-cell activation and autoimmunity in certain experimental settings, including transgenic expression of B7-H1 in β-cells of C57Bl/six mice (20–22). For these exceptions, an alternative receptor for B7-H1 has been proposed but not identified to date (23,24). We nevertheless felt that the weight of evidence, specifi-

cally in NOD mice, suggested that B7-H1 might serve as a tool to selectively suppress NOD pSC autoimmunity, allowing us to learn whether and how pSC cells impact on the β-cell autoimmune progression program: transgenic expression of B7-H1 in NOD β-cells protects from type 1 diabetes (19). We here describe the effects of a pSC B7-H1 transgene. Our finding of type 1 diabetes acceleration emphasizes the complexity of this costimulatory pathway, while the selective, intraislet CD8^{+} bias of high-affinity T-cells demonstrates that pSC cells do impact the β-cell destruction program, culminating in type 1 diabetes.

RESEARCH DESIGN AND METHODS

GFAP promoter–driven transgenic NOD mice. B7-H1 cDNA was derived by RT-PCR from NOD mouse splenocyte RNA and inserted into a GFAP expression cassette (Fig. 1*A*) (25). This construct was injected into fertilized

NOD ova, generating two independent male founders. One died young, with typical overt type 1 diabetes, before successful breeding. Positional cloning and sequencing indicated that the surviving founder carried the transgene on chromosome 12 (chr12:3302043.0.3202044, *Mus musculus*, build 37.1) in a noncoding region, not near known NOD type 1 diabetes risk loci. This founder and offspring developed and bred normally but had an immune phenotype (see below). NOD, NOD.*scid*, NOD-derived GFAP promoter–driven transgenic (GFAP-tg), and GFAP-tg.*scid* mice were generated and maintained under approved protocols in our vivarium. GFAP-tg.*scid* resembled NOD.*scid* in every respect, including normal pancreas histology and confocal immunofluorescence.

Surface plasmon resonance analysis. NOD B7-H1, from transgenic brain, or wild-type spleen were purified with a B7-H1 antibody (Cedarlane, Bullington, ON, Canada), coupled to an affinity column (GE Healthcare, Mississauga, ON, Canada). A CM5 Biacore chip was used to couple 200 response units of PD-1 (R&D Systems, Minneapolis, MN), and serial dilutions of purified B7-H1 (4.25–100 nmol/l) were injected. BIAevaluation software was used for analysis.

Histobiochemistry and image analyses. For insulitis quantitation, frozen tissue was processed, hemotoxilin-eosin–stained, and scored as previously described (4). Three-color immunofluorescence was used for confocal imaging of GFAP (in pSC and astrocytes), CD3, and insulin as previously described (4). For GFAP quantification studies, Volocity software was used; 68–100 islets/group were counted. Each individual islet perimeter was identified through islet autofluorescence and traced, and the total islet area was calculated (micrometers squared). The GFAP staining signal (fluoroisothiocyanate) of pSC was quantified within each islet by selective identification of "green" pSC and calculated as a percentage of GFAP-positive staining (in pixels) per total area of each islet, measured in micrometers squared. Image-J software was used to image the steric distribution of pSC loss, comparing GFAP green pixel counts in wild-type and transgenic islets of 8-week-old mice.

Cell preparations and transfers and in vitro studies. Spleen cells were prepared for intravenous injection or for in vitro cultures as previously described (4). Splenocytes (10^7) from NOD females with recent diabetes onset were injected intravenously into 8-week-old NOD.*scid* or GFAP-tg.*scid* recipients either treated or untreated with 200 μg i.p. mouse anti–B7-H1 antibody (R&D Systems) every second day. T-cell proliferation assays of splenocytes from 5- to 13-week-old NOD females were completed and analyzed as previously described (26). For DC antigen presentation analysis, 2×10^4 $CD11c^+$ GFAP-tg or wild-type NOD DCs were purified with a $CD11c^+$ selection kit (Stem Cell Technologies, Vancouver, BC, Canada) from spleens and cocultured with 2×10^5 T-cells purified with a $CD3^+$ selection kit (Stem Cell Technologies) from 10-week-old wild-type NOD mice and pulsed with insulin. For pancreatic lymph node T-cell proliferation assays, 2×10^5 lymphocytes from wild-type NOD or GFAP-tg animals were seeded with 2×10^5 irradiated splenocytes, pulsed with GFAP, processed, and analyzed as previously described (2).

T-cell and DC Studies. Pancreata were digested with collagenase (20′/37°C), dissociated, and applied to a Ficoll gradient. Islets were handpicked and cultured in leukocyte complete medium with 18 ng/ml interleukin-2 for 8 days prior to staining (5). Cells were stained for flow cytometry with anti-CD8 or anti-CD11c, CD11b, and/or B7-H1 and gated as indicated (e.g., $CD3^+$).

Diabetes monitoring. Blood glucose was measured twice weekly in animals ≥8 weeks old; measurements ≥13.8 mmol/l in two consecutive readings were considered diabetic. Insulin and glucose sensitivity and tolerance were measured as described (2).

Sialitis. hemotoxilin-eosin–stained submandibular salivary glands were scored by two blinded observers. Mononuclear foci were scored as "small" at <75 inflammatory cells/section and "large" at >75 inflammatory cells/section.

RESULTS

Characteristics of B7-H1 transgenic mice. B7-H1 expression was detected by transgene-specific RT-PCR in neuronal tissues, including brain and sciatic nerve, in pancreas but not in thymus or spleen (Fig. 1*B*). Traces of transgene transcripts were also found in colon and salivary glands. B7-H1 protein expression did not completely correlate with transcription profiles, which is not uncommon (27). Total B7-H1 protein expression was similar in transgenic and age- and sex-matched wild-type mice in most tissues examined but comparatively elevated in transgenic pSC cells and brain (Fig. S1, available in an

TABLE 1
Binding properties of B7-H1 and B7-H1 transgene (tg) to PD-1 receptor

Binding affinity	Surface plasmon resonance			
	K_d (nmol/l)	k_{on} ($\times 10^4$ mol · l^{-1} · sec^{-1})	k_{off} (sec^{-1})	R_{max} (RU)
B7-H1 → PD-1	11	16.7	0.0017	39.5
B7-H1 tg → PD-1	11	15.8	0.0017	36.4

K_d, equilibrium dissociation constant; k_{off}, dissociation constant; k_{on}, association constant; RU, resistance unit.

online appendix at http://diabetes.diabetesjournals.org/cgi/content/full/db09-1209/DC1). Confocal immunofluorescence colocalized GFAP and B7-H1 to transgenic pSC cells, with undetectable B7-H1 in wild-type pancreata (Fig. 1*C* and *D*). There was considerable transgene expression throughout the central nervous system in transgenic but not wild-type mice (Fig. 1*E* and *F*). Insular transgene expression in pSC did not generate endocrine malfunction, as analyzed by glucose and insulin sensitivity tests (Fig. S2). Transgene protein expression in colon and salivaries was at best very low and inconsistent in GFAP-tg mice (Fig. S1).

We compared binding affinities of purified wild-type PD-1 to wild-type and transgenic B7-H1 by surface plasmon resonance, with binding kinetics analyzed by 1:1 Langmuir binding isotherms (Fig. 1*G*; Table 1). No differences were identified, suggesting that the transgene ligates PD-1 normally. Collectively, these observations argue strongly that GFAP-tg phenotypes reflect B7-H1 costimulatory function in the islet locale rather than nonspecific transgenesis effects—a conclusion further supported by in vivo B7-H1 blocking studies (discussed below).

Type 1 diabetes development in GFAP-tg. As shown in Fig. 2*A*, transgenic mice progressed more rapidly to type 1 diabetes than wild-type females ($P = 0.0017$, life tables). More rapid pre-diabetes progression peaked by 19 weeks, with two-thirds of GFAP-tg diabetic compared with one-tenth of wild-type control mice. To begin exploring the mechanism of this counterintuitive phenotype, we quantified the progression of islet inflammation. The early phase of islet infiltration (peri-insulitis) was unaffected in transgenics ($P > 0.1$ vs. wild type) (Fig. 2*B*–*D*), but by 8 weeks of age, insulitis was much enhanced (Fig. 2*B*) and was more invasive in GFAP-tg mice compared with controls ($P < 0.001$) (Fig. 2*C*). Insulitis progression continued to accelerate (Fig. 2*C*) up to overt diabetes declaration ($P < 0.001$) (Fig. 2*D*).

Enhanced pSC loss in GFAP-tg. To determine whether increased insulitis severity correlated with accelerated pSC loss, a quantitative scoring system was developed. pSC integrity was measured as GFAP pixel-counts/islet cross-section. There was marked variation of islet sizes, but the distribution was similar in 8-week-old transgenic and wild-type mice, wild-type and transgenic NOD.*scid* mice, and 3-week-old wild-type or transgenic mice ($P > 0.1$) (Fig. 3*A*). However, the GFAP content (percentage of area) was much reduced in 8-week-old transgenics ($P < 0.0001$) (Fig. 3*B*). This loss was autoimmune mediated, given that GFAP-tg.*scid* (and very young animals) did not have GFAP loss ($P > 0.1$) (Fig. 3*B*). We used three-dimensional imaging to map the spatial distribution of pSC loss. As shown in Fig. 3*C*–*E*, transgenics clearly depleted
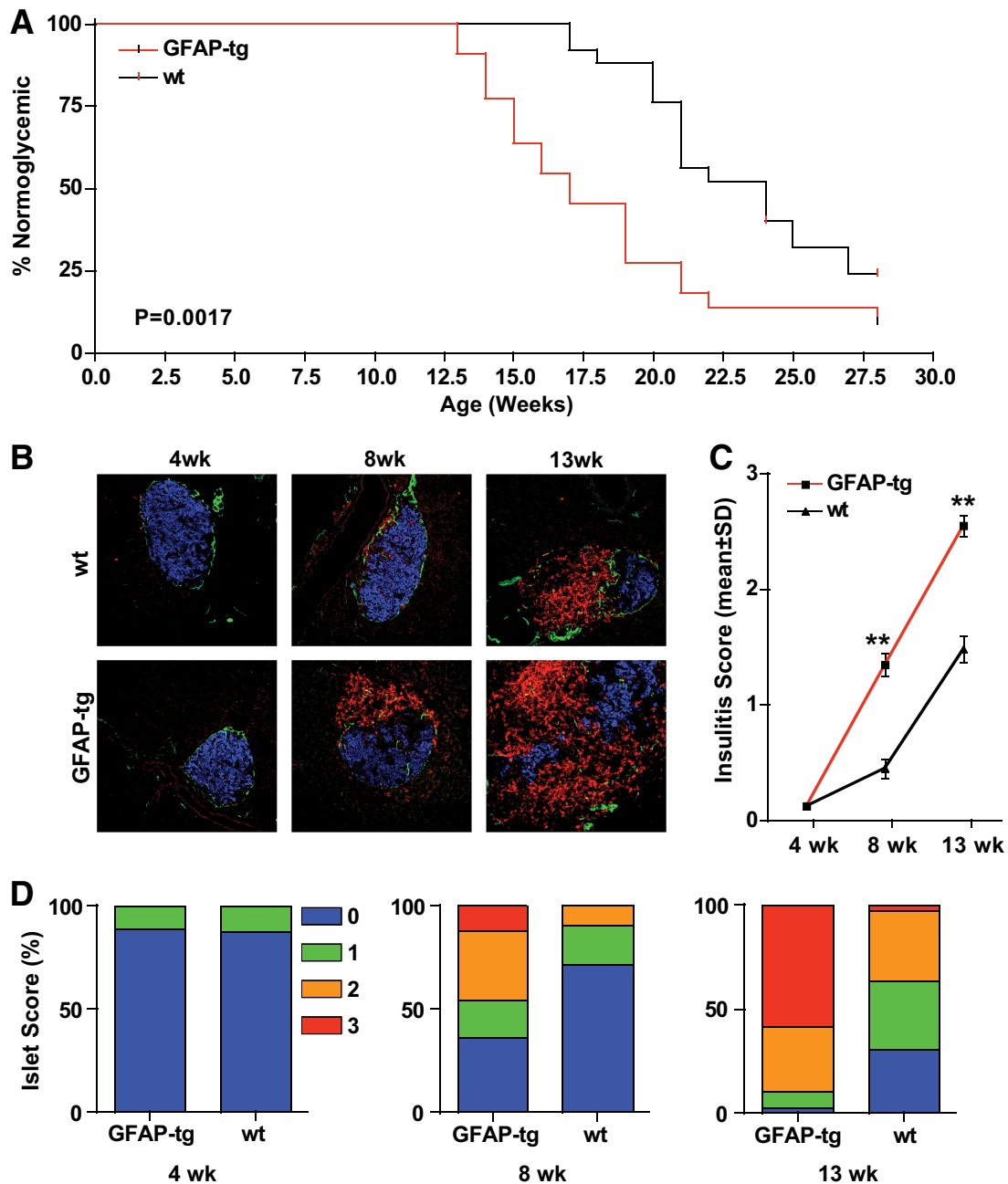
FIG. 2. Transgenic B7–H1 accelerates autoimmunity. *A*: Natural type 1 diabetes incidence in NOD females (wild-type [wt] NOD *N* = 25; GFAP-tg mice *N* = 22 [*P* = 0.006]). *B*: Histological analysis of wild-type and transgenic pancreata. Tissue was retrieved for immunohisto-chemistry at the ages indicated and stained for insulin (blue), GFAP (green), and CD3 (red). *C*: The progression of insulitis is significantly accelerated (*P* = 0.0001) in transgenics older than 4 weeks. **P* < 0.001. *D*: Distribution of insulitis scores over time (*N* = 8/group; *P* < 0.001 at 8 and 13 weeks). Scoring scale: 0 (blue), no insulitis; 1 (green), peri-insulitis; 2 (orange), 25–50% invasive islet damage; and 3 (red), >50% islet mass destroyed. There were ≥200 islets counted/mouse pancreas. wk, week. (A high-quality digital representation of this figure is available in the online issue.)

the pSC envelope by 8 weeks (Fig. 3*E*), while pSC integrity was maintained in young (Fig. 3*C*) as well as 8-week-old wild-type mice (Fig. 3*D*). Thus, several independent approaches, from histology to quantitative imaging, fully supported each other, and the addition of wild-type and transgenic NOD.*scid* mice added credibility to the notion that the transgenic phenotype reflects pSC impact on pre-diabetic autoimmunity.

Increased pathogenicity in GFAP-tg mice. Splenocytes from diabetic GFAP-tg donors transferred diabetes to wild-type NOD.*scid* recipients dramatically faster to more recipients than did wild-type diabetic donor cells (*P* =

0.023) (Fig. 4*A*; life tables), demonstrating that the transgene drives quantitative or qualitative immune changes that enhance the pathogenicity of systemic immune cells. Consistently, transfer of wild-type splenic grafts into transgenic NOD.*scid* recipients showed intermediate pathogenicity, with similar penetrance but slower pace of type 1 diabetes development in transgenic NOD.*scid* recipients (*P* = 0.02). Thus, these transfer data support those from natural history disease development (Fig. 2*A*), directly demonstrating type 1 diabetes acceleration in and by the transgenic islet.

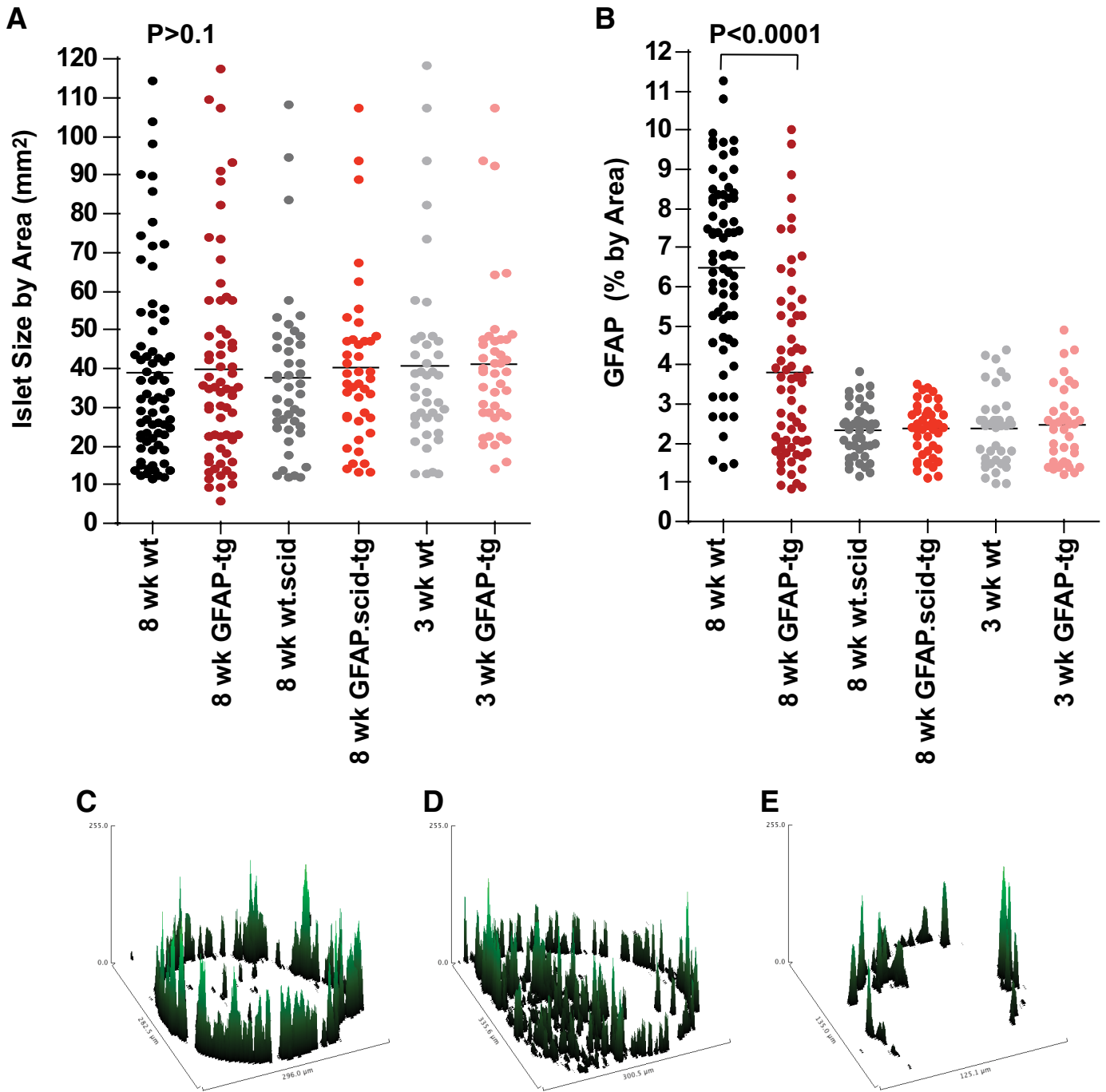The rapid adoptive transfer model facilitated studies of

FIG. 3. Transgenic B7–H1 expression accelerates pSC destruction. *A*: Islet size (cross-sectional measurements [micrometers squared]; $N = 67–72$). *B*: Depletion of islet GFAP content ($N = 67–72$/group). *C–E*: Three-dimensional imaging of GFAP pixel intensity in representative islets of wild-type (wt) NOD mice aged 5 (*C*) or 8 (*D*) weeks (wk) and of 8-week-old GFAP-tg NOD mice (*E*).

the role of B7-H1 function in wild-type and transgenic mice. Systemic blockade of B7-H1 by antibodies mediated acceleration and higher penetrance of type 1 diabetes development ($P = 0.02$) (Fig. 4*B*). In contrast, antibody blockade had no effects on the enhanced pathogenicity of transgenic grafts, indicating that the transferred pool of cells was no longer B7-H1 dependent ($P > 0.1$) (Fig. 4*C*). These results indicate that transgenic pSC cells influence local T-cells at the islet level, which are then recirculated into systemic distribution, refractory to further B7-H1 signals. In transgenics, this change is associated with cognate expansion of CD8$^+$ effector T-cells (as discussed below).

Enhanced T-cell selection in transgenic islets. To better understand the enhanced pathogenicity of autoreactive T-cell pools in transgenics, we compared in vitro proliferative recall responses to GFAP (pSC-cell specific) and insulin (β-cell specific; B9–23) (Fig. 5). T-cell reactivity to both autoantigens was observed in transgenic and wild-type mice. While insulin autoimmunity amplified, with pre-diabetes progression in both groups equally, transgenic GFAP recall responses peaked early and then declined and in fact differed significantly at every time point measured, with the decline in transgenics a good correlate of earlier pSC demise (Fig. 3*E*). Similarly, GFAP responses to the main NOD target epitope, GFAP p253–
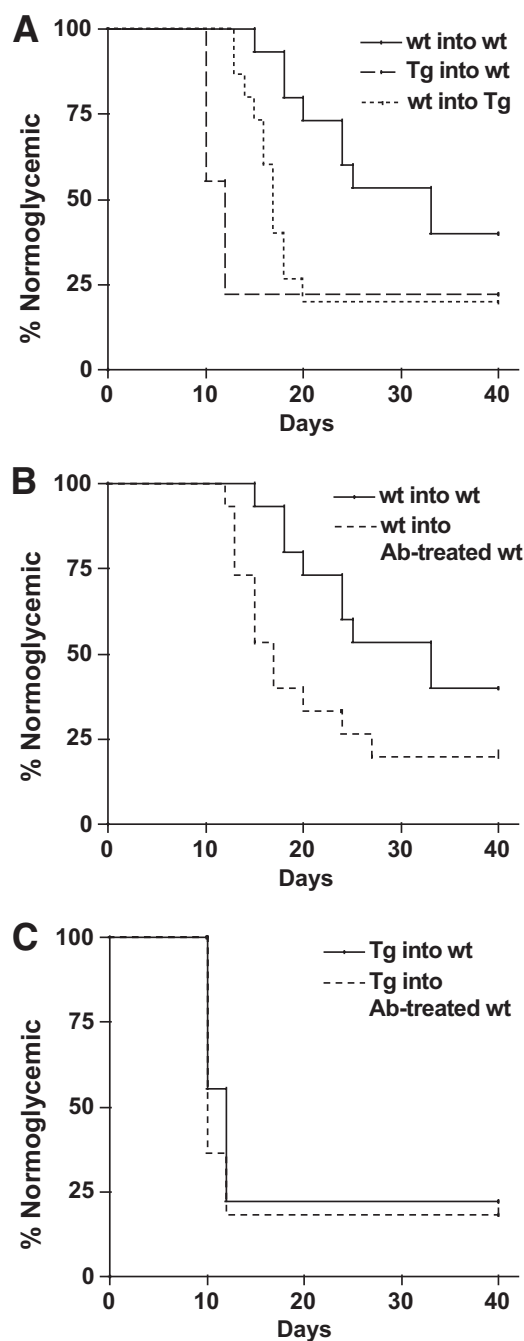
FIG. 4. Enhanced pathogenicity of GFAP-tg T-cells. *A*: Reciprocal adoptive transfers; injection of 15 × 10^6 splenocytes from diabetic donors into wild-type (wt) or transgenic (Tg) NOD.*scid* recipients as indicated in the figure (life table *P* values vs. wild type into wild-type NOD.scid: 0.031 for transgenic splenocytes into wild-type NOD.scid and 0.023 for wild-type into transgenic recipients). *B* and *C*: Similar adoptive transfers, adding animals receiving blocking doses of anti–B7–H1 antibody (Ab) on day 0 and every 2nd day of study. *B*: Antibody treatment accelerated type 1 diabetes development in wild-type recipients of wild-type splenocytes (*P* = 0.02). *C*: Anti–B7–H1 does not affect pathogenicity of Tg splenocytes in wild-type recipients (*P* > 0.1).

261 (5), were more pronounced at very low antigen concentrations, suggesting cognate selection of high-affinity T-cell receptors—again consistent with the more massive, early pSC damage (0.1 μg/ml, *P* = 0.020; 0.5 μg/ml, *P* = 0.015) (Fig. 5*C*). These observations suggest that the pSC transgene enhances the effectiveness of progressive pSC damage through more effective pSC-specific T-cell selection.

These data prompted us to compare T sublineage distribution in transgenic and wild-type mice. The different pre-diabetic tissues analyzed had similar numeric and proportionate T sublineage distributions in both mouse lines (Fig. 6*A* and *B*). However, a striking, transgene-driven phenotype was the islet-exclusive expansion of the proportions (*P* < 0.05) (Fig. 6*C*) and numbers of CD8$^+$ intraislet T-cell pool (*P* < 0.002). This independently supports the above conclusion that the pSC transgene imparts more pathogenic T-cell selection. There were no other changes in the cellular distributions, including B7-H1$^+$ dendritic cells (Fig. S3).

No transgene effects in early pre-diabetes. Autoimmune priming of (ultimately) pathogenic T-cells is thought to occur at a young age in pancreatic lymph nodes, where dendritic cells present fragments of apoptotic β-cell debris (28). There was not any evidence for more pronounced pSC cell (or β-cell) death in 3-week-old transgenic versus wild-type mice (Fig. 7*A* and *B*), with terminal deoxynucleotidyl transferase–mediated dUTP nick-end labeling–stained thymus tissue serving as a positive apoptosis control tissue (Fig. 7*C*). Absent GFAP-specific T-cell responses in pancreatic lymph node cells of the same animals provided a functional read-out for autoantigen unavailability at that time (Fig. 7*D*).

Early stages of the pre-diabetes progression program in these NOD females were thus not affected by the transgene, and enhanced number and pathogenicity of local autoreactive T-cells in transgenics likely reflected the local impact of positive costimulation by transgenic B7-H1. To rule out a dysfunction of DCs in this process, we purified DCs from transgenic and wild-type donors 3 weeks of age and used them to present antigen (insulin) to purified pre-diabetic (10 weeks old) wild-type T-cells (Fig. 7*E*). As shown, DCs from transgenic and wild-type donors performed as well as antigen-presenting cells.

The pSC transgene phenotype is pancreas selective. The NOD mouse develops two genetically independent, penetrant autoimmune disorders: type 1 diabetes and a primary Sjögren syndrome (29). Only if the transgene phenotype exclusively involved local costimulation in the islet would we expect the "the other autoimmune disease" (sialitis) to be unaffected. As shown in Fig. S4, sialitis proceeded at similar rates and with similar features in wild-type and GFAP-tg mice.

DISCUSSION

Systemic models (blocking or gene deletion) for the study of PD-1 and its ligand, B7-H1, have unequivocally shown dramatic effects on T-cell development (30–33), activation in lymphoid tissue (34,35), and modification of effector and regulatory T-cell functions in various tissue sites (36,37). With very few exceptions (20), PD-1 ligation is associated with negative costimulatory function, and an elusive, alternative B7-H1 receptor has been proposed, but not identified, for the exceptions (23,24). We sought to employ the negative costimulatory activity of B7-H1 to protect pSC cells from autoimmune destruction and thus obtain a tool to understand the pSC role in pre-diabetes progression. This failed because B7-H1 transgenic pSC accelerated disease development through selection of CD8$^+$-biased, more pathogenic, islet-resident T-cell pools. Our observations were more surprising because overexpression of B7-H1 in β-cells protected NOD mice from diabetes (19).
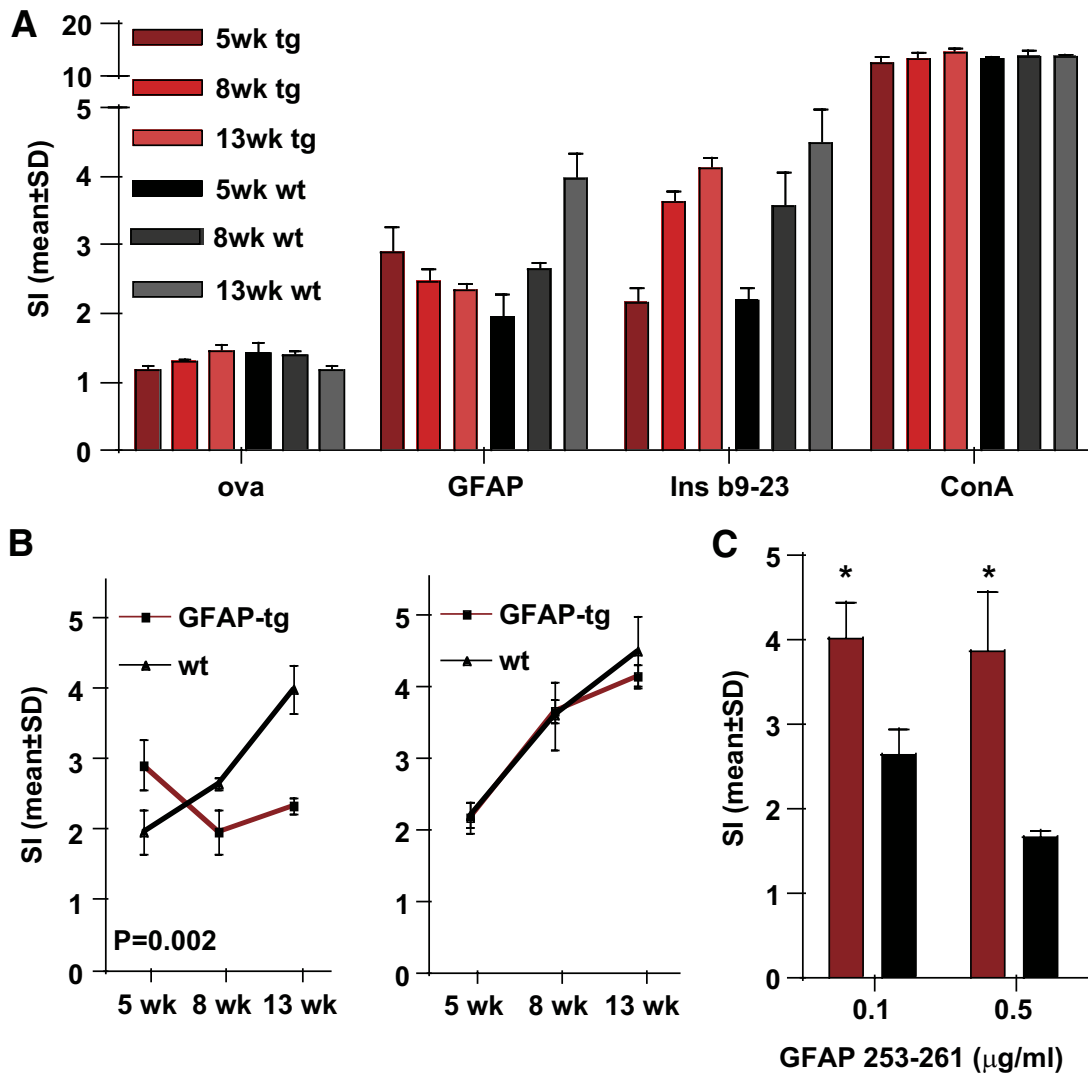
FIG. 5. Transgene effects on immune parameters. *A–C:* T-cell proliferation ($N = 5$ mice/group). *A*: Splenocytes (4×10^5/well) of wild-type (wt) or transgenic (tg) NOD mice aged 5–13 weeks (wk) were stimulated with whole GFAP, insulin peptide b9-23, or ovalbumin (ova). ConA, Concannavalin A. *B*: Time courses of GFAP *(left panel)* but not of insulin responses *(right panel)* differ between wild-type and transgenic mice ($P = 0.002$, ANOVA). *C*: Enhanced high-affinity T-cell responses to low concentrations of the major NOD GFAP peptide, p253–261, in wild-type (black bars) and 5-week-old transgenic (red bars) mice (*$P < 0.020$). SI, stimulation index (mean counts/minute unstimulated/stimulated).

However, a similar transgene in naturally type 1 diabetes–resistant C57BL/6 mice did generate diabetic mice (20). Current information is insufficient to explain these findings, but at the very least, one must conclude that expression of B7-H1 in nonhemopoietic tissue can bias local immune regulation and effector function either positively or negatively.

Irrespective of the molecular mechanisms that determine the outcome of tissue PD-1 ligation, our findings demonstrate an immunologically meaningful, disease-relevant interaction between T-cells and pSC cells in prediabetes. In GFAP-tg animals, severe pSC depletion by 8 weeks is the harbinger of rapid β-cell insufficiency. The selective numerical and proportionate expansion of CD8^{+} T-cells was exclusive to the islet locale, which is in line with the lack of major histocompatibility complex class II expression in pSC. The early peak of high-affinity, pSC-specific T-cell autoreactivity indicates that cognate events drive this T-cell expansion. Without concomitant rises in regulatory T-cells, these data delineate a cogent mechanism for type 1 diabetes acceleration, supported by the

sharing of type 1 diabetes–associated target autoantigens in pSC and β-cells (2,4).

The enhanced pathogenicity at type 1 diabetes onset, observed in adoptive transfer experiments, is then explained by systemic recirculation of the small islet T-cell pools. In vivo B7-H1 blocking studies suggested that these recirculated cells themselves are no longer influenced by B7-H1. This might actually contribute to their pathogenicity given that endogenous, negatively costimulating B7-H1 otherwise should have lessened the pathogenicity of these T-cells.

Other contributors to rapid β-cell loss likely include depletion of pSC neurotropic factors, a long-recognized pSC cell function (6–8). Thus, when transgenic and wild-type islets were compared, our data demonstrated that pSC actively modified the type 1 diabetes progression program—in the present case through the selection of more pathogenic anti-pSC T-cell reactivities.

One concern with any transgenic model is the creation or modification of a phenotype through insertional toxicity, postcloning transgene rearrangements, or nonphysi-
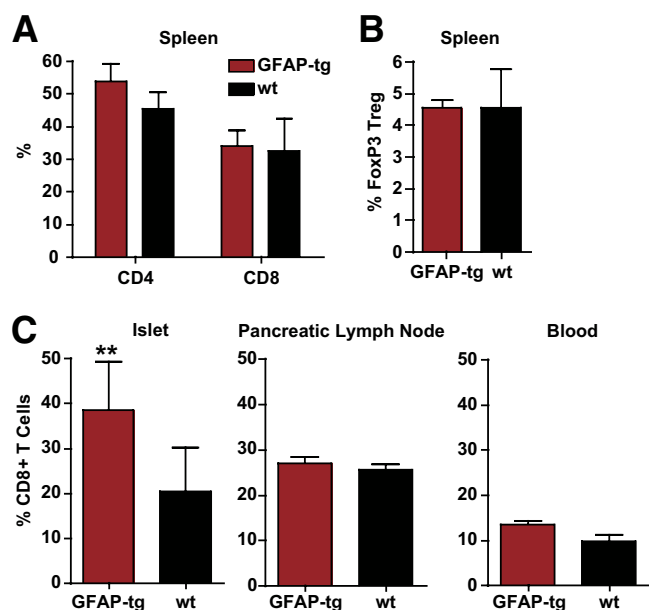
FIG. 6. Transgene-driven expansion of islet-invading CD8$^+$ T-cell pools. *A*: $n = 3$/group, $P > 0.1$. Cells were gated on CD3$^+$ T-cells. *B*: Splenic CD4$^+$CD25$^+$FoxP3$^+$ regulatory T-cell numbers remained unchanged in 8-week-old GFAP-tg mice. Cells were gated on CD3$^+$ T-cells. *C*: Islet-resident T-cells were isolated and expanded with interleukin-2 as described in RESEARCH DESIGN AND METHODS. Initial cell yields nearly doubled in transgenic islets, and the proportion of CD8$^+$ T-cells was enhanced compared with wild-type NOD mice (**$P = 0.048$). No differences in T sublineage proportions or numbers were observed in pancreatic lymph nodes, blood, or spleen. wt, wild type.

FIG. 7. No evidence for transgene-driven, preautoimmune pSC destruction. *A* and *B*: hemotoxilin-eosin/terminal deoxynucleotidyl transferase–mediated dUTP nick-end labeling stain in 3-week-old wild-type (*A*) or GFAP-tg (*B*) mice without evidence of early cell death. *C*: Positive TUNEL stain of thymus. *D*: Pancreatic lymph node cells (2×10^5) from 3-week-old GFAP-tg or wild-type NOD mice failed to respond to GFAP stimulation ($n = 3$/group; $P > 0.1$). White bar, ovalbumin; green bar, GFAP; black bar, Concannavalin A. *E*: Insulin auto-antigen presentation of CD11c$^+$ DCs purified from 3-week-old wild-type or GFAP-tg spleens. Cocultures of 2×10^4 DCs/well and 2×10^5 purified T-cells from 10-week-old wild-type NOD females were stimulated with insulin ($n = 3$/group; $P > 0.1$). White bar, ovalbumin; blue bar, insulin; black bar, Concannavalin A. wt, wild type. (A high-quality digital representation of this figure is available in the online issue.)

ological transgene expression levels. To rule out the possibility that the transgenic B7-H1 induced pSC apoptosis or affected islet physiology independently of T-cells, the transgene was crossed to lymphocyte-deficient NOD.*scid* mice. On the scid background, spontaneous diabetes was not observed and islets were indistinguishable from NOD.*scid* controls. In addition, the transgenic phenotype was faithfully transmitted in adoptive transfer studies, indicating its immune nature. Thus, the present observations establish that pSC cell–T-cell interactions directly impact diabetogenesis.

Rapid disease development in GFAP-tg mice reflects the selection of more pathogenic T-cell pools, skewed toward CD8$^+$ T-cells. Regulatory T-cells have been described to express the receptor for B7-H1 and PD-1 (37–39) and might be affected by the transgene expressed in the islet. However, the cellularity of CD4$^+$CD25$^+$FoxP3$^+$ T regulatory cells in GFAP-tg mice was not different by total numbers or proportions. Because of the very small absolute T regulatory numbers in the islet, we cannot exclude the possibility that they might be functionally suppressed by the islet transgene. This would then imply a coincidence of positive and negative costimulation in the same locale.

Collectively, the data now available cohesively support the conclusion that pSC cells are potent modulators of islet inflammation, able to shape the pre-diabetes progression program. Therapies that halt pSC damage should delay or reduce β-cell destruction, and innovative strategies for islet transplants, local β-cell regeneration, or de novo growth may benefit from the provision of pSC cell cografts derived from sural nerve fragments.
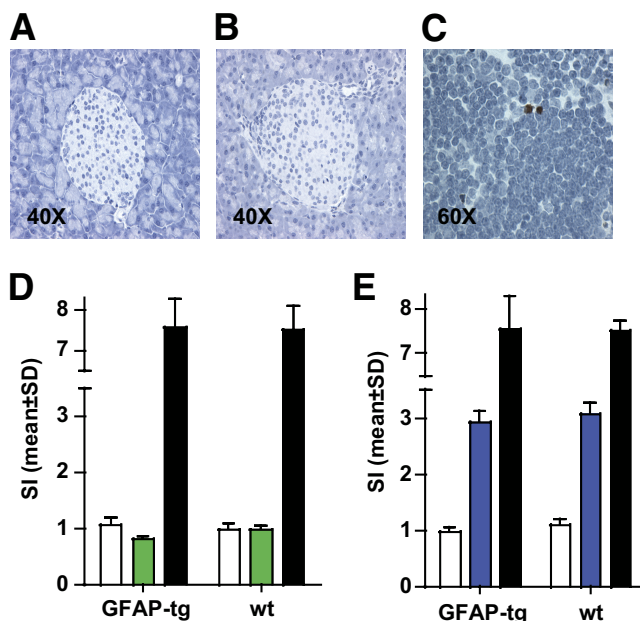
REFERENCES

1. Anderson MS, Bluestone JA. The NOD mouse: a model of immune dysregulation. Annu Rev Immunol 2005;23:447–485
2. Razavi R, Chan Y, Afifiyan FN, Liu XJ, Wan X, Yantha J, Tsui H, Tang L, Tsai S, Santamaria P, Driver JP, Serreze D, Salter MW, Dosch HM. TRPV1+ sensory neurons control beta cell stress and islet inflammation in autoimmune diabetes. Cell 2006;127:1123–1135
3. DiLorenzo TP, Graser RT, Ono T, Christianson GJ, Chapman HD, Roopenian DC, Nathenson SG, Serreze DV. Major histocompatibility complex class I-restricted T cells are required for all but the end stages of diabetes development in nonobese diabetic mice and use a prevalent T cell receptor alpha chain gene rearrangement. Proc Natl Acad Sci U S A 1998;95:12538–12543
4. Winer S, Tsui H, Lau A, Song A, Li X, Cheung RK, Sampson A, Afifiyan F, Elford A, Jackowski G, Becker DJ, Santamaria P, Ohashi P, Dosch HM. Autoimmune islet destruction in spontaneous type 1 diabetes is not beta-cell exclusive. Nat Med 2003;9:198–205
5. Tsui H, Chan Y, Tang L, Winer S, Cheung RK, Paltser G, Selvanantham T, Elford AR, Ellis JR, Becker DJ, Ohashi PS, Dosch HM. Targeting pancreatic glia in type 1 diabetes. Diabetes 2008;918–928
6. Vieira KP, de Almeida e Silva Lima Zollner AR, Malaguti C, Vilella CA, de Lima Zollner R. Ganglioside GM1 effects on the expression of nerve growth factor (NGF), Trk-A receptor, proinflammatory cytokines and on autoim-

mune diabetes onset in non-obese diabetic (NOD) mice. Cytokine 2008;42: 92–104

7. Mwangi S, Anitha M, Mallikarjun C, Ding X, Hara M, Parsadanian A, Larsen CP, Thule P, Sitaraman SV, Anania F, Srinivasan S. Glial cell line-derived neurotrophic factor increases beta-cell mass and improves glucose tolerance. Gastroenterology 2008;134:727–737

8. Casellas A, Salavert A, Agudo J, Ayuso E, Jimenez V, Moya M, Munoz S, Franckhauser S, Bosch F. Expression of IGF-I in pancreatic islets prevents lymphocytic infiltration and protects mice from type 1 diabetes. Diabetes 2006;55:3246–3255

9. Greenwald RJ, Freeman GJ, Sharpe AH. The B7 family revisited. Annu Rev Immunol 2005;23:515–548

10. Keir ME, Liang SC, Guleria I, Latchman YE, Qipo A, Albacker LA, Koulmanda M, Freeman GJ, Sayegh MH, Sharpe AH. Tissue expression of PD-L1 mediates peripheral T cell tolerance. J Exp Med 2006;203:883–895

11. Keir ME, Butte MJ, Freeman GJ, Sharpe AH 2008. PD-1 and its ligands in tolerance and immunity. Annu Rev Immunol 2008;26:677–704

12. Blank C, Mackensen A. Contribution of the PD-L1/PD-1 pathway to T-cell exhaustion: an update on implications for chronic infections and tumor evasion. Cancer Immunol Immunother 2007;56:739–745

13. Nakanishi J, Wada Y, Matsumoto K, Azuma M, Kikuchi K, Ueda S. Overexpression of B7–H1 (PD-L1) significantly associates with tumor grade and postoperative prognosis in human urothelial cancers. Cancer Immunol Immunother 2007;56:1173–1182

14. Iwai Y, Ishida M, Tanaka Y, Okazaki T, Honjo T, Minato N. Involvement of PD-L1 on tumor cells in the escape from host immune system and tumor immunotherapy by PD-L1 blockade. Proc Natl Acad Sci U S A 2002;99: 12293–12297

15. Ansari MJ, Salama AD, Chitnis T, Smith RN, Yagita H, Akiba H, Yamazaki T, Azuma M, Iwai H, Khoury SJ, Auchincloss H Jr, Sayegh MH. The programmed death-1 (PD-1) pathway regulates autoimmune diabetes in nonobese diabetic (NOD) mice. J Exp Med 2003;198:63–69

16. Salama AD, Chitnis T, Imitola J, Ansari MJ, Akiba H, Tushima F, Azuma M, Yagita H, Sayegh MH, Khoury SJ. Critical role of the programmed death-1 (PD-1) pathway in regulation of experimental autoimmune encephalomyelitis. J Exp Med 2003;198:71–78

17. Yao S, Chen L. Reviving exhausted T lymphocytes during chronic virus infection by B7–H1 blockade. Trends Mol Med 2006;12:244–246

18. Barber DL, Wherry EJ, Masopust D, Zhu B, Allison JP, Sharpe AH, Freeman GJ, Ahmed R. Restoring function in exhausted CD8 T cells during chronic viral infection. Nature 2006;439:682–687

19. Wang CJ, Chou FC, Chu CH, Wu JC, Lin SH, Chang DM, Sytwu HK. Protective role of programmed death 1 ligand 1 (PD-L1)in nonobese diabetic mice: the paradox in transgenic models. Diabetes 2008;57:1861–1869

20. Subudhi SK, Zhou P, Yerian LM, Chin RK, Lo JC, Anders RA, Sun Y, Chen L, Wang Y, Alegre ML, Fu YX. Local expression of B7–H1 promotes organ-specific autoimmunity and transplant rejection. J Clin Invest 2004; 113:694–700

21. Dong H, Zhu G, Tamada K, Chen L. B7–H1, a third member of the B7 family, co-stimulates T-cell proliferation and interleukin-10 secretion. Nat Med 1999;5:1365–1369

22. Tamura H, Dong H, Zhu G, Sica GL, Flies DB, Tamada K, Chen L. B7–H1 costimulation preferentially enhances CD28-independent T-helper cell function. Blood 2001;97:1809–1816

23. Wang S, Bajorath J, Flies DB, Dong H, Honjo T, Chen L. Molecular modeling and functional mapping of B7–H1 and B7-DC uncouple costimulatory function from PD-1 interaction. J Exp Med 2003;197:1083–1091

24. Shin T, Kennedy G, Gorski K, Tsuchiya H, Koseki H, Azuma M, Yagita H, Chen L, Powell J, Pardoll D, Housseau F. Cooperative B7–1/2 (CD80/CD86) and B7-DC costimulation of CD4+ T cells independent of the PD-1 receptor. J Exp Med 2003;198:31–38

25. Brenner M, Messing A. GFAP Transgenic Mice. Methods 1996;10:351–364

26. Winer S, Chan Y, Paltser G, Truong D, Tsui H, Bahrami J, Dorfman R, Wang Y, Zielenski J, Mastronardi F, Maezawa Y, Drucker DJ, Engleman E, Winer D, Dosch HM. Normalization of obesity-associated insulin resistance through immunotherapy. Nat Med 2009;15:921–929

27. Song A, Winer S, Tsui H, Sampson A, Pasceri P, Ellis J, Elliott JF, Dosch HM. Deviation of islet autoreactivity to cryptic epitopes protects NOD mice from diabetes. Eur J Immunol 2003;33:546–555

28. Hoglund P, Mintern J, Waltzinger C, Heath W, Benoist C, Mathis D. Initiation of autoimmune diabetes by developmentally regulated presentation of islet cell antigens in the pancreatic lymph nodes. J Exp Med 1999;189:331–339

29. Winer S, Astsaturov I, Cheung R, Tsui H, Song A, Gaedigk R, Winer D, Sampson A, McKerlie C, Bookman A, Dosch H-M. Prevention of primary Sjögren's syndrome by ICA69-deficiency. Lancet 2002;360:1063–1069

30. Keir ME, Latchman YE, Freeman GJ, Sharpe AH. Programmed death-1 (PD-1):PD-ligand 1 interactions inhibit TCR-mediated positive selection of thymocytes. J Immunol 2005;175:7372–7379

31. Blank C, Brown I, Marks R, Nishimura H, Honjo T, Gajewski TF. Absence of programmed death receptor 1 alters thymic development and enhances generation of CD4/CD8 double-negative TCR-transgenic T cells. J Immunol 2003;171:4574–4581

32. Nishimura H, Honjo T, Minato N. Facilitation of beta selection and modification of positive selection in the thymus of PD-1-deficient mice. J Exp Med 2000;191:891–898

33. Nishimura H, Agata Y, Kawasaki A, Sato M, Imamura S, Minato N, Yagita H, Nakano T, Honjo T. Developmentally regulated expression of the PD-1 protein on the surface of double-negative (CD4-CD8-) thymocytes. Int Immunol 1996;8:773–780

34. Edgtton KL, Kausman JY, Li M, O'Sullivan K, Lo C, Hutchinson P, Yagita H, Holdsworth SR, Kitching AR. Intrarenal antigens activate CD4+ cells via CO-stimulatory signals from dendritic cells. J Am Soc Nephrol 2008;19: 515–526

35. Keir ME, Freeman GJ, Sharpe AH. PD-1 regulates self-reactive CD8+ T cell responses to antigen in lymph nodes and tissues. J Immunol 2007;179: 5064–5070

36. Kitazawa Y, Fujino M, Wang Q, Kimura H, Azuma M, Kubo M, Abe R, Li XK. Involvement of the programmed death-1/programmed death-1 ligand pathway in CD4+CD25+ regulatory T-cell activity to suppress alloimmune responses. Transplantation 2007;83:774–782

37. Raimondi G, Shufesky WJ, Tokita D, Morelli AE, Thomson AW. Regulated compartmentalization of programmed cell death-1 discriminates CD4+CD25+ resting regulatory T cells from activated T cells. J Immunol 2006;176:2808–2816

38. Tsui H, Winer S, Jakowsky G, Dosch HM. Neuronal elements in the pathogenesis of type 1 diabetes. Rev Endocr Metab Disord 2003;4:301–310

39. Polanczyk MJ, Hopke C, Vandenbark AA, Offner H. Treg suppressive activity involves estrogen-dependent expression of programmed death-1 (PD-1). Int Immunol 2007;19:337–343